Proc. Natl. Acad. Sci. USA
Vol. 96, pp. 9821–9826, August 1999
Medical Sciences

Noninvasive quantitation of cytosine deaminase transgene expression in human tumor xenografts with *in vivo* magnetic resonance spectroscopy

LAUREN D. STEGMAN*, ALNAWAZ REHEMTULLA†, BRADLEY BEATTIE‡, ELS KIEVIT†, THEODORE S. LAWRENCE†, RONALD G. BLASBERG‡, JURI G. TJUVAJEV‡, AND BRIAN D. ROSS*§

Departments of *Radiology and Biological Chemistry and †Radiation Oncology, University of Michigan Medical School, 1150 West Medical Center Drive, MSRBIII Room 9301 Ann Arbor, MI 48109-0648; and ‡Department of Neurology, Memorial Sloan Kettering Cancer Center, 1275 York Avenue K 293, New York, NY 10021

Communicated by J. L. Oncley, University of Michigan, Ann Arbor, MI, June 11, 1999 (received for review March 1, 1999)

ABSTRACT **Analysis of transgene expression *in vivo* currently requires destructive and invasive molecular assays of tissue specimens. Noninvasive methodology for assessing the location, magnitude, and duration of transgene expression *in vivo* will facilitate subject-by-subject correlation of therapeutic outcomes with transgene expression and will be useful in vector development. Cytosine deaminase (CD) is a microbial gene undergoing clinical trials in gene-directed enzyme prodrug gene therapy. We hypothesized that *in vivo* magnetic resonance spectroscopy could be used to measure CD transgene expression in genetically modified tumors by directly observing the CD-catalyzed conversion of the 5-fluorocytosine (5-FC) prodrug to the chemotherapeutic agent 5-fluorouracil (5-FU). The feasibility of this approach is demonstrated in subcutaneous human colorectal carcinoma xenografts in nude mice by using yeast CD (yCD). A three-compartment model was used to analyze the metabolic fluxes of 5-FC and its metabolites. The rate constants for yCD-catalyzed prodrug conversion (k_1^{app}), 5-FU efflux from the observable tumor volume (k_2^{app}), and formation of cytotoxic fluorinated nucleotides from 5-FU (k_3^{app}) were 0.49 ± 0.27 min^{-1}, 0.766 ± 0.006 min^{-1}, and 0.0023 ± 0.0007 min^{-1}, respectively. The best fits of the 5-FU concentration data assumed first-order kinetics, suggesting that yCD was not saturated *in vivo* in the presence of measured intratumoral 5-FC concentrations well above the *in vitro* K_m. These results demonstrate the feasibility of using magnetic resonance spectroscopy to noninvasively monitor therapeutic transgene expression in tumors. This capability provides an approach for measuring gene expression that will be useful in clinical gene therapy trials.**

Gene-directed enzyme-prodrug therapy (GDEPT) is designed to overcome the dose-limiting systemic toxicity of cancer chemotherapy by expressing nonmammalian enzymes in tumor cells that convert low-toxicity prodrugs to cytotoxic metabolites. The success of GDEPT obviously depends on adequate distribution and expression of the therapeutic transgene in the target tumor. Analysis of transgene expression in GDEPT protocols has traditionally necessitated invasive assays on tissue specimens. A noninvasive method for monitoring the location, magnitude, and duration of transgene expression would be of considerable value. Such an assay would facilitate development of vector technology and allow subject-by-subject correlation of therapeutic efficacy with levels of transgene expression.

Magnetic resonance spectroscopy (MRS) may be an effective, noninvasive method for monitoring *in vivo* expression of the cytosine deaminase (CD, EC 3.5.4.1) GDEPT transgene, which is currently in clinical trials (1). CD is a microbial enzyme that catalyzes the conversion of the low-toxicity antifungal agent 5-fluorocytosine (5-FC) to the antimetabolite 5-fluorouracil (5-FU). Mammalian cells lack CD activity, and localizing microbial CD to tumors can be an effective means of achieving localized production of 5-FU, a broad-spectrum drug widely used in the chemotherapy of solid tumors. Animal studies suggest that CD-mediated conversion of 5-FC may prove to be a powerful strategy for overcoming the dose-limiting systemic toxicity of 5-FU and improving its poor objective response rate of 5–25% (2). The prodrug conversion reaction catalyzed by CD should be MRS-observable because 5-FC and its major metabolites are fluorinated, and ^{19}F produces a strong MRS signal with no background from endogenous compounds.

^{19}F-MRS is clinically available in a number of centers and has proven useful for monitoring the metabolism and pharmacokinetics of fluorinated drugs. The broad chemical shift range of fluorine also results in good separation of fluoropyrimidine drugs and their metabolites (3). ^{19}F-MRS has been used extensively to study the effects of radiation (4), biochemical modulation (5–7), and regional infusion (8) on 5-FU metabolism (9). The quantitative nature of *in vivo* ^{19}F-MRS measurements has been confirmed with HPLC (10, 11). Building on previous MRS studies of 5-FC metabolism in perfused yeast cultures (12–16), conversion of 5-FC to 5-FU by antibody–yeast CD conjugates has been observed with MRS (17).

The *Saccharomyces cerevisiae* CD (yCD) gene was recently cloned (18–20). We have demonstrated that yCD is therapeutically superior to *Escherichia coli* CD, which has been historically used in CD-GDEPT protocols (20). In this study, we demonstrate the effective use of ^{19}F-MRS for noninvasive *in vivo* quantitation of yCD gene expression in animals. Conversion of 5-FC to 5-FU was observed in subcutaneous human HT29 colon carcinoma xenoplants expressing yCD (20). Pharmacokinetic modeling of 5-FC conversion to 5-FU and the subsequent clearance and metabolism of 5-FU by endogenous enzymes based on dynamic ^{19}F-MRS data yielded measurements of yCD gene expression and the rate of fluoronucleoside synthesis in each of the animals. These results suggest that ^{19}F-MRS assessment of yCD gene expression and fluoronucleoside synthesis could provide useful information in the design and evaluation of human trials with yCD/5-FC tumor gene therapy.

MATERIALS AND METHODS

Cell Culture and Animal Model. Human HT29 colon carcinoma cells were obtained from American Type Culture

Abbreviations: MRS, magnetic resonance spectroscopy; GDEPT, gene directed enzyme-prodrug therapy; CD, cytosine deaminase; 5-FC, 5-fluorocytosine; 5-FU, 5-fluorouracil; FNuc, fluorinated nucleosides/nucleotides; FβAl, fluoro-β-alanine; yCD, yeast cytosine deaminase.

§To whom reprint requests should be addressed. E-mail: bdross@umich.edu.

The publication costs of this article were defrayed in part by page charge payment. This article must therefore be hereby marked "*advertisement*" in accordance with 18 U.S.C. §1734 solely to indicate this fact.

PNAS is available online at www.pnas.org.

Collection and grown as described (21). The HT29/yCD cell line stably expressing *S. cerevisiae* CD has been previously characterized (20). Female nude mice (*Nu/Nu* CD-1, Charles River Breeding Laboratories), 7–8 weeks old, were injected subcutaneously in the rear limbs with 5×10^6 viable tumor cells.

***In Vitro* ^{19}F-MRS.** HT29/yCD cells were grown in 10-cm dishes to subconfluence. Cells were then incubated in growth medium containing 5 mM 5-FC or 5-FU (Sigma). After 3 hr, conditioned medium and cell pellets were collected and frozen at −70°C. Conditioned media and sonicated cell extracts were subsequently dried, and the residues were resuspended in 0.5 ml ^2H_2O with 5 mM NaF. Spectra were acquired on a 7T Bruker NMR-spectrometer with a single-pulse sequence, a 90° flip angle, 5 s repetition time, 16,384 data points over a 22-kHz spectral width, WALTZ16 broad-band decoupling, and 64 transients.

***In Vivo* ^{19}F-MRS.** All experiments were approved by the University of Michigan committee for animal use. Animals with tumors ≈250 mm^3 ($n = 5$) were briefly anesthetized with isofluorane, given an intraperitoneal dose of 1 g/kg 5-FC, and restrained on a specially constructed plastic jig that immobilizes the tumor-bearing hind limb (22). The conscious mouse was then positioned so that the tumor was directly under the surface coil and placed at the isocenter of the magnet. This procedure, including optimizing the magnetic field homogeneity to a typical proton line width of 20–60 Hz and tuning the coil to the fluorine frequency, required approximately 20 min. Spectra were then acquired every 20 min for a minimum of 3 hr. Local conversion of 5-FU was confirmed by repositioning animals ($n = 3$) to acquire spectra from muscle on the contralateral limb.

^{19}F-MR spectra were obtained at 282.3 MHz by using on a Varian Unity Inova system equipped with a 7T, 18.3-cm horizontal bore magnet. A custom-built, 6.1-mm diameter, single-turn circular surface coil tunable to both the proton (300.7 MHz) and fluorine frequencies was used as a transmitter and receiver. Spectra were acquired as the average of 277 transients (free induction decays) collected in 8,192 data points by using a 25-μs pulse width (corresponding to a 90° flip angle at a depth of 2.7 mm), 4.328-ms repetition time, and a 25-kHz spectral width; 20 min were required for each spectrum. The pulse repetition time used was greater than five times the reported T_1 of 5-FU and its metabolites in whole blood (6, 23); thus, no saturation of the metabolites of interest was expected. This was empirically verified by varying the repetition time in a single animal after 5-FC injection and comparing the signal intensities from limited number of signal averages. A microcell containing NaF in normal saline was placed just above the surface coil to provide an external chemical shift and concentration standard. The transmitter frequency was offset to place the center of the spectrum midway between the NaF and fluoro-β-alanine (FβAl) resonance frequencies. Each spectrum was apodized with a 60-Hz exponential line-broadening function before Fourier transformation, individually phased, and baseline corrected with a cubic spline method by using the VNMR software (Varian). Metabolite resonance areas were quantified with a spectral deconvolution and integration routine and were normalized to that of the external reference standard. To determine absolute intratumoral metabolite concentrations, a scaling factor relating the NaF signal in the microcell to the fluorine signals arising from the tumor volume was used. The scaling factor was obtained from MRS experiments by using the NaF external standard microcell and a tumor phantom containing a known concentration of 5-FC in normal saline.

Serum Pharmacokinetics. Serum 5-FC concentrations were determined by using GC/MS. After i.p. administration of 5-FC, animals ($n = 3$ per time point) were killed by rapid cervical dislocation and blood was obtained by cardiac puncture. 5-Chlorouracil was added to aliquots of serum (100 μl) as an internal standard. Subsequently, samples were prepared for GC/MS as described (24). Serum levels were determined by comparing the ratio of summed areas of the 5-FC and 5-chlorouracil ion peaks to a calibration curve obtained from a least-squares linear regression fit (typical $r^2 = 0.99$) of serum spiked with known concentrations of 5-FC and 5-chlorouracil.

Pharmacokinetic Modeling. A compartmental model describing the kinetics of 5-FC, 5-FU, and fluorinated nucleosides/nucleotides (FNuc) in HT29/yCD tumors is shown in Fig. 1. It consists of three compartments, 5-FC in tissue, 5-FU in tissue, and FNuc in tissue. The "tissue" space, as defined in this model, combines the interstitial and intracellular spaces. Two factors support this simplification: (*i*) the high transport rate between these two spaces of both 5-FC and 5-FU relative to the rate of change of concentration of the of the compounds within the spaces and (*ii*) the extra- to intracellular distribution volumes for 5-FC and 5-FU are both close to unity (unpublished data).

^{19}F-MRS measures concentrations within this tissue space plus a contribution from the vascular space. The volume of the vascular space in tumors is relatively small (1–4%) (25). Scaling the serum 5-FC concentration curve by this volume suggests that the effect of the vascular space on the measured tissue 5-FC concentration should be small. Similarly, the lack of significant levels of 5-FU and FNuc in the blood should not effect the tissue measurements.

When 5-FC or 5-FU become bound, either in an enzyme–substrate complex or to other compounds within the tissue, they no longer contribute to the (5-FC or 5-FU) peak in the ^{19}F-MR spectra. It is assumed that the total amount of bound 5-FC and 5-FU at any point in time is negligibly small, because the concentration of binding proteins in the tumor volume is unlikely to be above a few millimolar and the rate of fluorinated nucleotide incorporation into RNA is slow (23). Thus, the ^{19}F-MRS measurements can be assumed to reflect the concentrations within the tissue space.

In this model, the term k_1 governs the rate of yCD-catalyzed conversion of 5-FC into 5-FU. Similarly, k_3 describes the rate of production of FNuc from 5-FU by the combined action of uridine phosphorylase and uridine kinase. The term k_2 defines the rate of efflux of nonmetabolized 5-FU out of the tissue. Because there is uncertainty regarding the actual intracellular concentration of 5-FC convertible by 5-FC, all values for derived rate constants are expressed as apparent. Two variants of this model were developed and applied to the data, one that assumes first-order kinetics (i.e., nonsaturable) throughout, and another which assumes that the k_1^{app} and k_3^{app} conversion processes are saturable at concentrations defined by *in vitro* determined Michaelis–Menten constants for the corresponding enzymes. In the first variant, the rate of conversion of 5-FC to 5-FU is equal to k_1[5-FC] whereas in the second variant, the conversion rate is equal to $(k_1[\text{5-FC}])/(K_m + [\text{5-FC}])$; where K_m is the *in vitro* Michaelis–Menten constant for yCD.

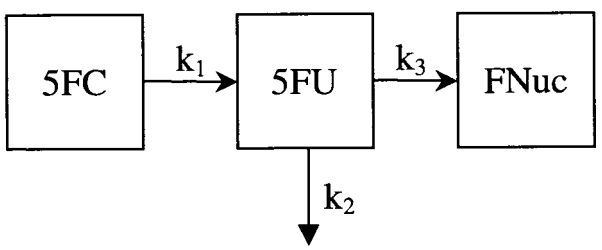

FIG. 1. Schematic representation of the 3-compartment model used in the pharmacokinetic analysis of 5-FC metabolism in yCD-transduced human tumor xenografts. The compartmental transfer constants are k_1^{app} and k_3^{app}; k_2^{app} is an elimination rate constant.

Both model variants also assume the following: (*i*) the effect of the serum concentration of 5-FC on the measured tissue concentration of 5-FC is negligible; (*ii*) the effect of bound 5-FC and 5-FU on the measured tissue concentrations of 5-FC and 5-FU is negligible; (*iii*) distribution of 5-FC and 5-FU between interstitial and intracellular spaces is effectively instantaneous with a distribution volume of 1.0; (*iv*) the concentrations of 5-FC, 5-FU, and FNuc within the compartments is homogeneous; (*v*) the transport of 5-FU out of the tissue has first-order kinetics and is the same for each of the animals studied here; (*vi*) measured levels of 5-FU and FNuc are due solely to intratumoral production; (*vii*) the production of 5-FU and FNuc are both unidirectional; and (*viii*) FNuc is effectively trapped within the tumor tissue.

The transport of 5-FU across cell membranes is believed to be by passive or facilitated diffusion (26), and the efflux of 5-FU out of tumor tissue should be passive and similar for tumors in different animals. Because of the slow rate of change of 5-FC concentration observed in these experiments, it was difficult to determine k_2^{app} reliably from a single animal's data set. Therefore, a single shared k_2^{app} parameter was used for all five animals and all were fitted simultaneously, each with their own k_1^{app} and k_3^{app} parameters.

Estimates of the parameters were determined by using a constrained nonlinear least-squares search algorithm (MATLAB version 5.2, Mathworks, Natick, MA). Solutions to the equations of the first-order model were determined analytically. For the saturation kinetics model, the solutions to the differential equations were determined numerically by using the Runge–Kutta method of Dormand and Prince (49).

RESULTS

Conversion of 5-FC to 5-FU was observed in HT29/yCD tumors. Serial spectra demonstrating the time course of 5-FC metabolism in a representative HT29/yCD tumor are shown in Fig. 2. Each displayed spectrum was averaged over a 20-min interval; spectral acquisition was initiated 20 min after i.p. injection of 5-FC. Both 5-FC and 5-FU resonances were observed in the first spectrum. The intratumoral concentration of 5-FC peaked approximately 40 min postadministration, whereas the peak 5-FU concentration lagged slightly, occurring in the 60-min spectrum. Anabolism of 5-FU by endogenous enzymes produced a small FNuc peak, which was first observable 40 min after 5-FC administration. The intensity of the intracellularly trapped FNuc peak grew continuously over the time course of the experiment. The chemical shifts of the fluorine metabolites were in good agreement with those reported in the literature (23, 27). Localized production of 5-FU in HT29/yCD tumors was confirmed by obtaining spectra from contralateral muscle, where only 5-FC was observed ($n = 3$).

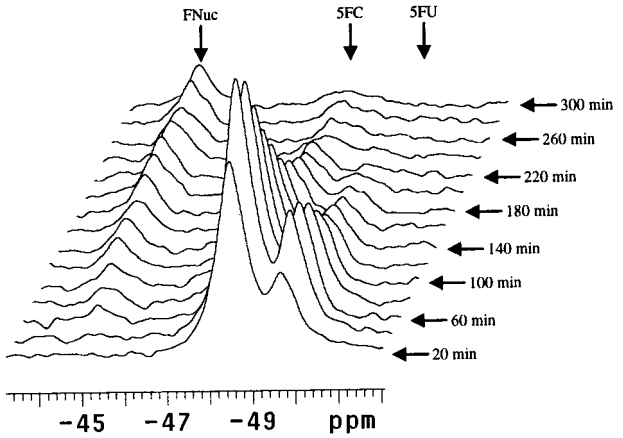

FIG. 2. Serial ^{19}F spectra of a subcutaneous HT29/yCD tumor. Acquisition began 20 min after i.p. administration of 1 g/kg 5-FC. Each spectrum is the average of 277 free induction decays collected in a 20-min interval. The time from 5-FC injection to the beginning of the acquisition interval are shown beside the spectra. The chemical shift assignments (in ppm) of the metabolite peaks relative to NaF are: FNuc, −45.0; 5-FC, −48.5; and 5-FU, −49.6.

No conversion of 5-FC to 5-FU was observed in five nontransduced HT29 tumors (Fig. 3*A*). In addition, catabolism of 5-FU to FβAl was observed in two of five animals with HT29/yCD tumors (Fig. 3*B*). In a separate study, we determined whether HT29 cells directly produce FβAl. The cells were cultured in the presence of 5-FC or 5-FU for 3 h, and the conditioned medium and cell extracts were analyzed with high-resolution ^{19}F-MRS. FβAl was not detected in parental or HT29/yCD cells after treatment with 5-FC or 5-FU *in vitro*.

Serum 5-FC concentrations in tumor-free mice were determined with GC/MS. The i.p. injection resulted in a slow rate of change in 5-FC concentration in the blood. The maximal serum 5-FC concentration of 7.2 ± 0.1 mM was achieved 45 min after i.p. injection. The clearance of 5-FC from serum could be described by a single exponential with half-time of 44.7 min. These pharmacokinetic properties are consistent with those reported for 5-FC in the same mouse strain (28).

A slow rate of change in 5-FC concentration in the tissue was also observed, because tissue levels follow those in blood. This made it difficult for the model to accurately estimate k_2^{app}. Because the estimate of k_1^{app} covaries with that of k_2^{app}, an accurate estimate of k_2^{app} is needed if absolute quantitation of k_1^{app} is to be obtained. For situations in which a relative measure of k_1^{app} is sufficient, a simplified, equilibrium-type experimental protocol could be used involving a slow 5-FC infusion. If k_3^{app} is much smaller than k_2^{app}, and it is assumed that k_2^{app} is approximately the same in different studies, then a single-time-point MRS measurement of the [5-FU]/[5-FC] concentration ratio should reflect the relative expression of yCD. Under this condition, the generation of parametric chemical shift MRS images of yCD expression should be feasible.

The parameters describing the metabolism and distribution of 5-FC and its metabolites were calculated by using two different versions of a kinetic model described in *Materials and*

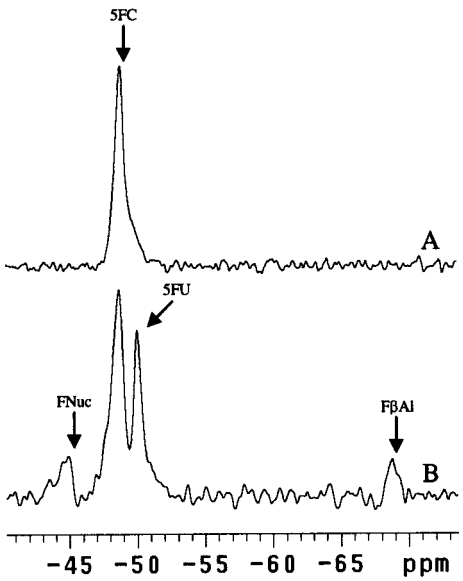

FIG. 3. Representative ^{19}F spectra from subcutaneous tumors obtained 120–150 min after i.p. injection of 1 g/kg 5-FC. (*A*) Untransduced HT29 carcinoma. (*B*) HT29/yCD carcinoma. The chemical shift of FβAL relative to NaF is −68.2 ppm.

Methods. The fit of the 5-FC/5-FU data determined by the model incorporating saturation kinetics, based on the Michaelis–Menten constant determined for yCD from *in vitro* studies, was unsatisfactory (Fig. 4*A*, dashed line). To achieve good fits with this model, a significantly larger value (>10 mM) for K_m of yCD would be necessary, thus making it roughly equivalent to a first-order process at the concentration of 5-FC measured in the tumors. Fig. 4*A* also shows a fit of the same 5-FC/5-FU data from a model that assumes first-order kinetics (solid line). Fits of the FNuc time course with both the first-order and saturation-kinetics versions of the model were equally good (Fig. 4*B*). The FNuc data were too noisy to distinguish between the two kinetic models. This distinction, however, had a negligible affect on the value of the parameter governing the rate of conversion of 5-FC to 5-FU (i.e., k_1^{app}, the parameter of interest). Table 1 summarizes the kinetic constants derived from the application of the first-order model to fit the animal data. The average k_1^{app} value in the 5 animals was 0.49 ± 0.27 min^{-1}, k_2^{app} was 0.766 ± 0.006 min^{-1}, and k_3^{app} was 0.0023 ± 0.0007 min^{-1}.

The combination of rate constants, $K_i = k_1^{app} \times k_3^{app}/(k_2^{app} + k_3^{app})$, reflects the overall reaction rate for 5-FC conversion to 5-FU and FNuc, assuming first-order kinetics. K_i can also be obtained from a graphical plot of the 5-FC and FNuc data as shown in Fig. 5 by using Patlak analysis (29). A graphical estimate of K_i was obtained for each animal and is shown in Table 1. The K_i^{app} values correspond well to the $k_1^{app} \times k_3^{app}/(k_2^{app} + k_3^{app})$ values. Thus, the rate of FNuc synthesis (μmol·$time^{-1}$·unit $volume^{-1}$) in yCD/5-FC treated tumors can be calculated from knowledge of K_i^{app} and 5-FC concentration in the tissue.

DISCUSSION

Interest in noninvasive methods for measuring therapeutic transgene expression is increasing as the clinical application of gene therapy expands. Work in this area has focused on developing reporter gene systems that can be monitored by positron-emission tomography, SPECT, or MRI (30–35). Chemical-shift selective imaging of the distribution of 5-FU and its metabolites is feasible (36). The ability of MRS to follow prodrug conversion dynamically and to distinguish between individual metabolites is a significant advantage over positron-emission tomography methods, which require measurement of plasma metabolite levels and must rely on selective trapping of radiolabeled 5-FC metabolites in transduced cells (37). The characteristics of MRS technology allow quantitation of yCD activity and simultaneous assessment of 5-FU catabolism and anabolism in yCD-transduced tumors. This quantitative assessment does not require blood sampling, because the concentrations of the precursor can be directly and simultaneously measured in the tissue. As a result, multiple input and response functions can be determined by sequential MRS, thereby greatly enhancing the constraints on the model parameters.

In this study, we have demonstrated the ability of noninvasive ^{19}F-MR spectroscopy to follow the metabolism of 5-FC and quantitate yCD expression in animals bearing subcutaneous tumors expressing yCD. Because the 5-FC concentrations achieved in these experiments did not sufficiently saturate tumor yCD activity, we could not place an upper limit on the value of K_m^{app} *in vivo*. Thus, a linear model was used to provide a reasonable approximation of 5-FC kinetics. The model suggests that the K_m^{app} for yCD *in vivo* is significantly larger than the value determined *in vitro* (20). Similar observations of log-order or more differences in the K_m values determined *in vitro* and *in vivo* have been reported in positron-emission tomography ligand–neuroreceptor binding studies (38, 39).

The higher *in vivo* K_m^{app} of yCD may be partially attributed to the fact that MRS measures concentrations in the total tumor space, including 5-FC in the tumor interstitium and vasculature, which is sequestered from conversion by intracellular yCD. A recent study by using MRS techniques capable of distinguishing between intra- and extracellular 5-FU demonstrated that a fraction of intratumoral 5-FU after i.v. administration of 5-FU remains in the extracellular space (40). It is likely that a fraction of the observed intratumoral 5-FC is in the extracellular space. Heterogeneous distribution of 5-FC throughout the tumor may also result in a higher *in vivo* K_m^{app} because of the averaging of saturating concentrations in some regions and low concentrations in other regions. Variations in 5-FU concentrations have been observed after 5-FU administration (36, 41). Experiments to map the distribution of 5-FC within tumors and to distinguish between intra- and extracellular drug will address the contributions of these effects to the higher *in vivo* K_m^{app} of yCD. Guanyl and thymidyl nucleobases are potent mixed competitive/noncompetitive allosteric inhibitors of yCD (42). Such inhibition may contribute to the higher K_m^{app} of yCD *in vivo* and suggests that mutating this allosteric site may produce a more efficient *in vivo* 5-FC convertase.

The MRS-based assessment of yCD/5-FC gene therapy may provide useful prognostic information that could help guide the clinical management of individual patients. Pharmacokinetic modeling of the MRS data can yield estimates of indi-

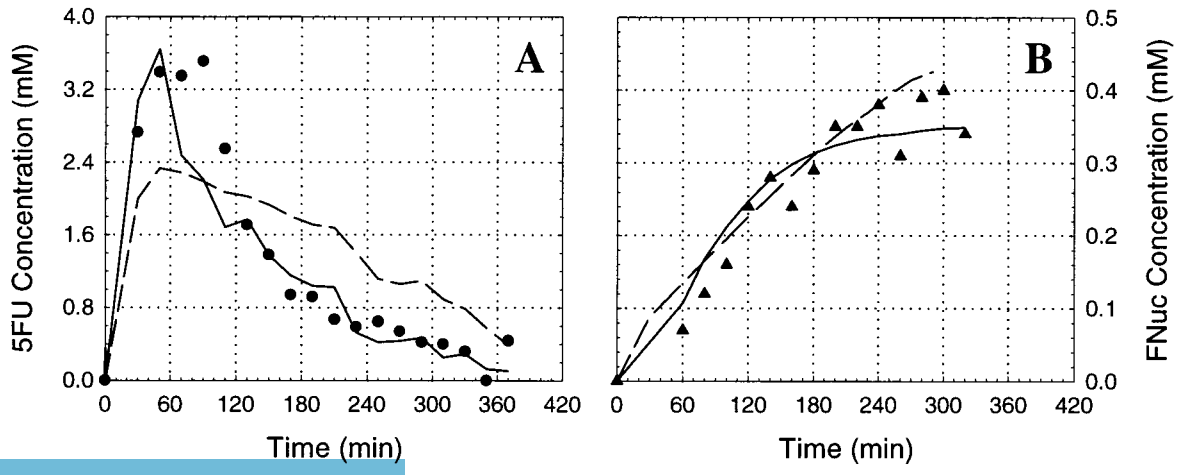

FIG. 4. Pharmacokinetic analysis of 5-FC anabolites in a representative HT29/yCD tumor. The MRS-determined concentrations of 5-FU (*A*) and FNuc (*B*) were fit by using two independent pharmacokinetic models. The first (broken lines) assumes saturation kinetics and the second (solid lines) assumes first-order kinetics.

Table 1. Kinetic constants derived from fitted data

Rat	k_1^{app}	k_3^{app}	$\frac{k_1^{app} \times k_3^{app}}{(k_2^{app} + k_3^{app})}$	K_i^{app}
1	0.316	0.0029	0.0012	0.0090
2	0.831	0.0023	0.0025	0.0018
3	0.728	0.0010	0.0010	0.0009
4	0.287	0.0022	0.0008	0.0010
5	0.267	0.0028	0.0010	0.0011
Overall	0.4860 ± 0.27	0.0023 ± 0.0007	0.0013 ± 0.0007	0.0028 ± 0.0035

$k_2^{app} = 0.766 \pm 0.006$

Overall values are given as mean ± SD.

vidual rate constants in the model. An estimate of the overall rate $[k_1^{app} \times k_3^{app}/(k_2^{app} + k_3^{app})]$ for the conversion of 5-FC to FNuc was also obtained, and it was shown that graphical analysis yields a similar value (K_i^{app}). The agreement of the Patlak analysis with the first-order pharmacokinetic model further supports the conclusion that yCD is in fact not saturated *in vivo*. Although graphical analysis does not yield separate estimates of k_1^{app} and k_3^{app}, it is statistically more robust and simple to implement. K_i^{app} is the parameter of therapeutic interest, because FNuc mediates the cytotoxicty of yCD/5-FC therapy by inhibiting thymidylate synthase and blocking DNA synthesis. Tumors with a low K_i^{app} would be expected to respond poorly to yCD/5-FC therapy. The relationship between $K_i^{app} \times$ [5-FC] and treatment response in yCD/5-FC protocols needs to be explored further.

The rate constant k_2^{app} is substantially larger than k_3^{app}; this means that the rate of 5-FU clearance from tumor tissue is faster than the rate of FNuc synthesis and accumulation in tumor tissue ($k_2^{app}/k_3^{app} > 200$). The calculated residence half-time of 5-FU in HT29/yCD tumors was only 0.9 min, reflecting the high value of k_2^{app}. This explains the unsuccessful attempts to image CD activity in CD-expressing tumors in rats with [^{18}F]5-FU and positron-emission tomography as reported previously (37). Namely, the failure to produce images of CD activity occurred because there was minimal entrapment of ^{18}F-labeled FNuc products in tumor cells during the period of imaging. Our results also are consistent with previous clinical MRS studies demonstrating a significant association between the intratumoral half-life of 5-FU and therapeutic response (43–45).

The accumulation of FβAl, a hepatic catabolite of 5-FU, was observed in two of the five HT29/yCD tumors. HT29 cells are derived from a human colon carcinoma, thus the appearance

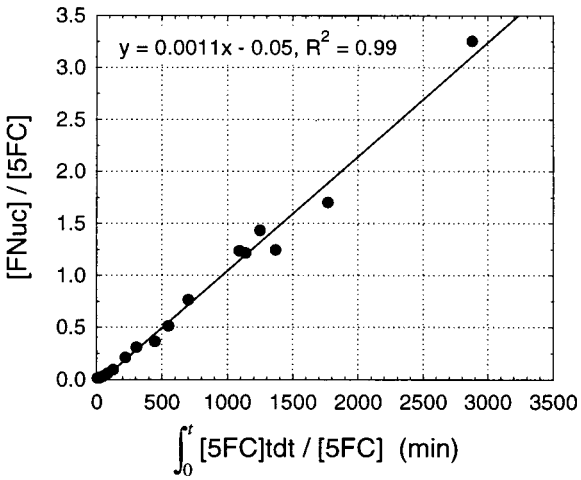

FIG. 5. Patlak analysis of a representative animal. The net accumulation of FNuc in the tumor (moles FNuc·min^{-1}·mole^{-1} 5-FC) is determined graphically by the slope of the time-dependence of the linearized 5-FC and FNuc tissue concentrations.

of a metabolite peak at the specific resonance of FβAl was unexpected. The lack of FβAl production by HT29/yCD cells in the presence of 5-FC or 5-FU *in vitro* implies that the FβAl observed *in vivo* was not produced by the tumor cells themselves. This is consistent with previously reported ^{19}F-MRS observations of 5-FU metabolism in perfused cultures of HT29 cells (46). Because FβAl production occurs almost exclusively in hepatocytes (47), we suggest that 5-FU produced in the tumor may enter the systemic circulation. The liver extracts ≈85% of the 5-FU present in blood at each passage (9) and converts it to FβAl, which is returned to the blood. Prior *et al.* (48) observed that systemically administered FβAl accumulates in subcutaneous tumors. Such a hepatic cycle may account for the observed FβAl production in two animals with HT29/yCD tumors. In support of this hypothesis, we recently found 19.7 ± 6.6 μM 5-FU ($n = 6$) in the serum of animals harboring HT29/yCD tumors 90 min after i.p. administration of 1 g/kg 5-FC. In addition, a 15% weight loss was observed in mice carrying a heavy bilateral HT29/yCD tumor burden after four daily i.p. doses of 500 mg/kg 5-FC (unpublished data). The lack of visible 5-FC conversion in muscle contralateral to the tumors confirms that the yCD GDEPT approach does result in "localized" chemotherapy despite the leakage of minute quantities of 5-FU into the systemic circulation. In fact, such leakage may correlate with the degree of "bystander effect" killing of neighboring untransduced tumor cells.

Recently, we demonstrated that yCD is therapeutically superior to *E. coli* CD in the treatment of HT29 tumor xenografts (20). The results of this study further support this conclusion; 5-FC conversion and FNuc accumulation was observed only in HT29/yCD tumors and in none of five HT29 tumors stably expressing *E. coli* CD (data not shown). The inability to observe 5-FC conversion in HT29/bCD tumors with ^{19}F-MRS is likely because of the 17.9 ± 4.4 mM K_m of the bacterial enzyme, which is well above the maximal 5-FC concentrations measured in both tumors and serum following a 1 g/kg dose. These results also support the hypothesis that yCD therapeutic efficacy depends on the efficiency of 5-FU and FNuc production.

In conclusion, this study demonstrates the ability of MRS to noninvasively estimate the level of yCD gene expression and the synthesis of FNuc synthesis *in vivo.* Pharmacokinetic modeling adds an important dimension and is particularly useful for MRS, because simultaneous measurements of precursor and product concentrations provide the opportunity to define multiple input and response functions. More importantly, the model parameters $[k_1^{app} \times k_3^{app}/(k_2^{app} + k_3^{app})]$ and tumor 5-FC concentration may be predictive of therapeutic response to yCD/5-FC treatment. MRS studies obtained over the course of yCD/5-FC treatment could help guide tumor transduction schedules and 5-FC doses. The growing availability of high-field animal and human MRS instruments will make ^{19}F-MRS techniques more practical for optimizing yCD gene therapy and assessing improvements in vector technology. Although we have applied ^{19}F-MRS to specifically estimate CD gene expression, in principle, similar MRS methodologies could be developed for other gene therapy paradigms.

We thank Drs. Michael Garwood and Thomas L. Chenevert for helpful comments. This work was supported in part by research grants from the National Institutes of Health to B.D.R. (CA59009), A.R. (CA73904), and T.S.L. (CA80145).

1. Crystal, R. G., Hirschowitz, E., Lieberman, M., Daly, J., Kazam, E., Henschke, C., Yankelevitz, D., Kemeny, N., Silverstein, R., Ohwada, A., *et al.* (1997) *Hum. Gene Ther.* **8,** 985–1001.
2. Calabresi, P. & Chabner, B. (1995) in *Goodman and Gilman's The Pharmacological Basis of Therapeutics*, eds. Hardman, L., Limbird, P., Molinoff, P., Ruddon, R. & Gilman, A. (Pergamon, New York), pp. 1225–1287.
3. McSheehy, P. & Griffiths, J. (1989) *NMR Biomed.* **2,** 122–141.
4. Blackstock, A. W., Kwock, L., Branch, C., Zeman, E. M. & Tepper, J. E. (1996) *Int. J. Radiat. Oncol. Biol. Phys.* **36,** 641–648.
5. McSheehy, P. M., Robinson, S. P., Ojugo, A. S., Aboagye, E. O., Cannell, M. B., Leach, M. O., Judson, I. R. & Griffiths, J. R. (1998) *Cancer Res.* **58,** 1185–1194.
6. Holland, S. K., Bergman, A. M., Zhao, Y., Adams, E. R. & Pizzorno, G. (1997) *Magn. Reson. Med.* **38,** 907–916.
7. Findlay, M. P., Leach, M. O., Cunningham, D., Collins, D. J., Payne, G. S., Glaholm, J., Mansi, J. L. & McCready, V. R. (1993) *Ann. Oncol.* **4,** 597–602.
8. Blesing, C. H. & Kerr, D. J. (1996) *J. Drug Target* **3,** 341–347.
9. Wolf, W., Waluch, V. & Presant, C. A. (1998) *NMR Biomed.* **11,** 380–387.
10. Findlay, M., Raynaud, F., Cunningham, D., Iveson, A., Collins, D. & Leach, M. (1994) *Ann. Oncol.* **7,** 47–53.
11. Newell, D. R., Maxwell, R. J. & Golding, B. T. (1992) *NMR Biomed.* **5,** 273–278.
12. Vialaneix, J. P., Chouini, N., Malet-Martino, M. C., Martino, R., Michel, G. & Lepargneur, J. P. (1986) *Antimicrob. Agents Chemother.* **30,** 756–762.
13. Di Vito, M., Podo, F., Torosantucci, A., Carpinelli, G., Whelan, W. L., Kerridge, D. & Cassone, A. (1986) *Antimicrob. Agents Chemother.* **29,** 303–308.
14. Whelan, W. L. (1987) *Crit. Rev. Microbiol.* **15,** 45–56.
15. Chouini-Lalanne, N., Malet-Martino, M. C., Martino, R. & Michel, G. (1989) *Antimicrob. Agents Chemother.* **33,** 1939–1945.
16. Fasoli, M. O., Kerridge, D., Morris, P. G. & Torosantucci, A. (1990) *Antimicrob. Agents Chemother.* **34,** 1996–2006.
17. Aboagye, E. O., Artemov, D., Senter, P. D. & Bjujwalla, Z. M. (1998) *Cancer Res.* **58,** 4075–4078.
18. Erbs, P., Exinger, F. & Jund, R. (1997) *Curr. Genet.* **31,** 1–6.
19. Hayden, M. S., Linsley, P. S., Wallace, A. R., Marquardt, H. & Kerr, D. E. (1998) *Protein Expression Purif.* **12,** 173–184.
20. Kievit, E., Bershad, E. M., Ng, E. Y., Sethna, P., Dev, I., Lawrence, T. S. & Rehemtulla, A. (1999) *Cancer Res.* **59,** 1417–1421.
21. Lawrence, T. S., Davis, M. A., Maybaum, J., Stetson, P. L. & Ensminger, W. D. (1990) *Radiat. Res.* **123,** 192–198.
22. Lyons, J., Ross, B. & Song, C. (1992) *Int. J. Radiat. Oncol. Biol. Phys.* **25,** 95–103.
23. El-Tahtawy, A. & Wolf, W. (1991) *Cancer Res.* **51,** 5806–5812.
24. Lawrence, T. S., Davis, M. A., Maybaum, J., Mukhopadhyay, S. K., Stetson, P. L., Normolle, D. P., McKeever, P. E. & Ensminger, W. D. (1992) *Cancer Res.* **52,** 3698–3704.
25. Nakagawa, H., Groothuis, D. R., Owens, E. S., Patlak, C. S., Pettigrew, K. D. & Blasberg, R. G. (1988) *J. Neurooncol.* **6,** 157–168.
26. Domin, B. A., Mahony, W. B. & Zimmerman, T. P. (1993) *Biochem. Pharmacol.* **46,** 503–510.
27. Malet-Martino, M. C., Martino, R., de Forni, M., Andremont, A., Hartmann, O. & Armand, J. P. (1991) *Infection* **19,** 178–180.
28. Huber, B. E., Austin, E. A., Good, S. S., Knick, V. C., Tibbels, S. & Richards, C. A. (1993) *Cancer Res.* **53,** 4619–4626.
29. Patlak, C. S., Blasberg, R. G. & Fenstermacher, J. D. (1983) *J. Cereb. Blood Flow Metab.* **3,** 8–32.
30. Tjuvajev, J. G., Stockhammer, G., Desai, R., Uehara, H., Watanabe, K., Gansbacher, B. & Blasberg, R. G. (1995) *Cancer Res.* **55,** 6126–6132.
31. Tjuvajev, J. G., Finn, R., Watanabe, K., Joshi, R., Oku, T., Kennedy, J., Beattie, B., Koutcher, J., Larson, S. & Blasberg, R. G. (1996) *Cancer Res.* **56,** 4087–4095.
32. Tjuvajev, J. G., Avril, N., Oku, T., Sasajima, T., Miyagawa, T., Joshi, R., Safer, M., Beattie, B., DiResta, G., Daghighian, F., *et al.* (1998) *Cancer Res.* **58,** 4333–4341.
33. Bogdanov, A., Jr., & Weissleder, R. (1998) *Trends Biotechnol.* **16,** 5–10.
34. Gambhir, S. S., Barrio, J. R., Wu, L., Iyer, M., Namavari, M., Satyamurthy, N., Bauer, E., Parrish, C., MacLaren, D. C., Borghei, A. R., *et al.* (1998) *J. Nucl. Med.* **39,** 2003–2011.
35. Jacobs, A., Dubrovin, M., Hewett, J., Sena-Esteves, M., Tan, C., Slack, M., Sadelain, M., Breakefield, X. O. & Tjuvajev, J. G. (1999) *Neoplasia* **1,** 154–161.
36. Brix, G., Bellemann, M. E., Gerlach, L. & Haberkorn, U. (1999) *Magn. Reson. Imaging* **17,** 151–155.
37. Haberkorn, U., Oberdorfer, F., Gebert, J., Morr, I., Haack, K., Weber, K., Lindauer, M., van Kaick, G. & Schackert, H. K. (1996) *J. Nucl. Med.* **37,** 87–94.
38. Gatley, S. J., Ding, Y. S., Brady, D., Gifford, A. N., Dewey, S. L., Carroll, F. I., Fowler, J. S. & Volkow, N. D. (1998) *Nucl. Med. Biol.* **25,** 449–454.
39. Kawai, R., Carson, R. E., Dunn, B., Newman, A. H., Rice, K. C. & Blasberg, R. G. (1991) *J. Cereb. Blood Flow Metab.* **11,** 529–544.
40. Brix, G., Belleman, M. E., Gerlach, L. & Haberkorn, U. (1998) *Radiology* **209,** 259–267.
41. Brix, G., Bellemann, M. E., Haberkorn, U., Gerlach, L., Bachert, P. & Lorenz, W. J. (1996) *Nucl. Med. Biol.* **23,** 897–906.
42. Ipata, P. L., Marmocchi, F., Magni, G., Felicioli, R. & Polidoro, G. (1971) *Biochemistry* **10,** 4270–4276.
43. Schlemmer, H. P., Bachert, P., Semmler, W., Hohenberger, P., Schlag, P., Lorenz, W. J. & van Kaick, G. (1994) *Magn. Reson. Imaging* **12,** 497–511.
44. Presant, C. A., Wolf, W., Albright, M. J., Servis, K. L., Ring, R. d., Atkinson, D., Ong, R. L., Wiseman, C., King, M., Blayney, D., *et al.* (1990) *J. Clin. Oncol.* **8,** 1868–1873.
45. Wolf, W., Presant, C. A., Servis, K. L., el-Tahtawy, A., Albright, M. J., Barker, P. B., Ring, R. d., Atkinson, D., Ong, R., King, M., *et al.* (1990) *Proc. Natl. Acad. Sci. USA* **87,** 492–496.
46. Malet-Martino, M. C., Faure, F., Vialaneix, J. P., Palevody, C., Hollande, E. & Martino, R. (1986) *Cancer Chemother. Pharmacol.* **18,** 5–10.
47. Maehara, Y., Nagayana, S., Okazaki, H., Nakamura, H., Shirasaka, T. & Fuji, S. (1981) *Gann* **72,** 824–827.
48. Prior, M. J. W., Maxwell, R. J. & Griffiths, J. R. (1990) *Biochem. Pharmacol.* **39,** 857–863.
49. Dormand, J. R. & Prince, P. J. (1980) *J. Comput. Appl. Math.* **6,** 19–26.